Implications for the split mission scenario

Robin J. Hogan* **Anthony J. Illingworth**

Department of Meteorology, University of Reading, UK.
***Email: R.J.Hogan@reading.ac.uk**

INTRODUCTION

It has been suggested that financial constraints may exclude the possibility of a payload of two active instruments on a cloud profiling satellite, and that work should be carried out to determine whether or not dividing the instruments between two satellites in very close orbits would severely reduce the accuracy of size retrievals. It has been shown that a second satellite could trail the first with the footprints drifting towards and away from each other by as much as 5 km.

In this paper synthetic cloud fields are generated with the same spectral characteristics as those observed by ground based radars, the spaceborne radar and lidar are 'flown' across the field with varying footprint separation, and the changes in the measured radar/lidar backscatter ratio are simulated as a function of footprint separation. A mean ice particle size can be derived from the radar/lidar backscatter ratio in cirrus provided this ratio is not affected by footprint separation.

GENERATION OF SYNTHETIC CLOUD FIELDS

In order to estimate the magnitude of the errors arising from non co-located footprints we need to know the typical spatial structure of real cirrus clouds. This information has been obtained using vertically-pointing ground-based 35 and 94 GHz observations at Chilbolton, England. Ten second averages of reflectivity factor were recorded with a vertical resolution of 75 m. Averaging was performed to reduce the vertical resolution to 525 m, close to the 500 m proposed for a spaceborne radar. A number of 1024-point time-series of reflectivity factor (in dBZ) in cirrus were selected, and the temporal scale converted to a spatial scale using a simple Taylor transformation and the mean wind speed over Chilbolton at that time and altitude as diagnosed by the UK Meteorological Office Unified Model. Only time-series in which all points registered cloud were considered. Information on the horizontal structure was then obtained by fitting power laws of the form

$$E = E_0 \, k^{\mu} \tag{1}$$

to the Fourier spectra of these data, where k is wavenumber, E is power spectral density, and E_0 and μ are constants. The best fit lines were least squares fits in log-log space after 7-point averaging of the spectra to reduce scatter. The parameter μ was found to vary between -1.8 and -2.4 in cirrus, which compares with the range -1 to -2 found by Danne et al. (1996). A spectrum typical of those analysed is shown in Fig. 1. It had the form $E = 2.03 \times 10^{-5} k^{-2.16}$ dBZ^2 m (where k is in m^{-1}), and we will use this from now on.

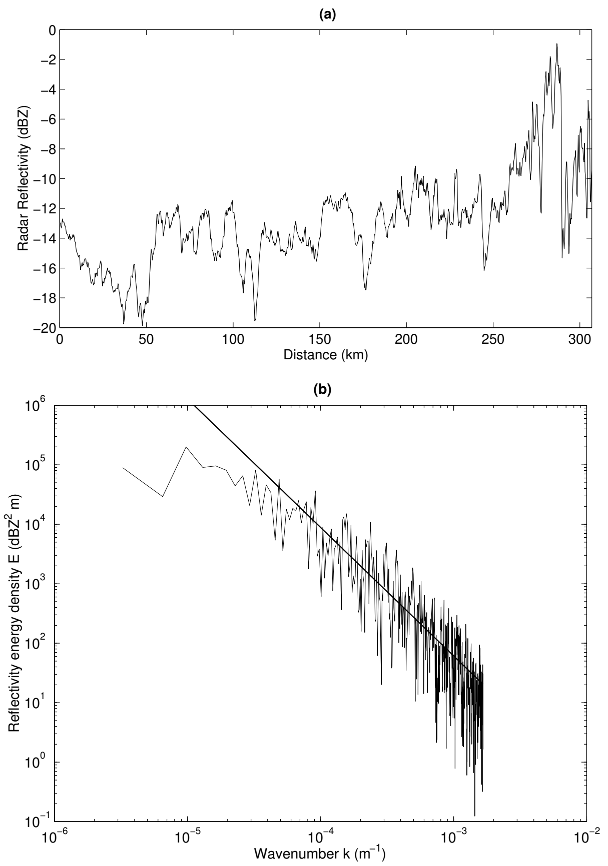

Fig. 1: (a) 35 GHz reflectivity factor at an altitude of 7 km. The abscissa has been converted from time to space using a mean wind at this altitude of 30 m s^{-1}. (b) The corresponding power spectrum. The best fit line is $E = 2.03 \times 10^{-5} k^{-2.16}$.

Cloud fields were generated by calculating the inverse two-dimensional Fourier transform of synthetic matrices containing wave amplitudes consistent with the energy at the various scales indicated by the one-dimensional spectrum. The phase of each wave component of the matrix was random, so that each cloud field was different. The domains were square and measured 25.6 km on a side with a resolution of 100 m. Fourier analysis of cross-sections through the domain confirmed that they had almost identical spectral properties as the original data. An example is shown in Fig. 2. Note that these cloud fields are spectrally isotropic, whereas real cirrus clouds with fallstreaks are not because the fallstreaks tend to be aligned parallel to the vertical wind-shear vector. On average this is not

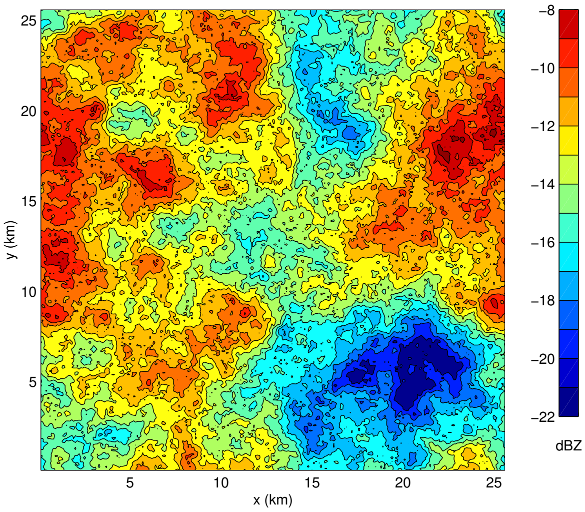

Fig. 2: Example of a simulated two-dimensional cloud field.

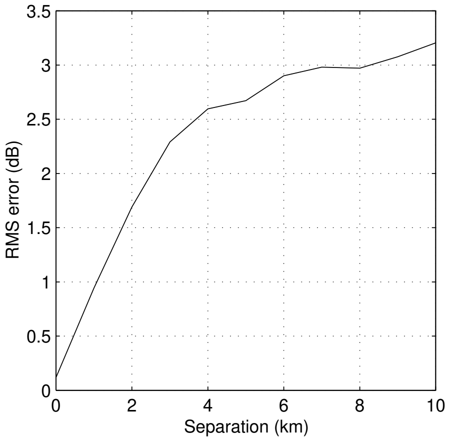

Fig. 3: RMS error in the lidar/radar backscatter ratio as a function of footprint separation.

expected to significantly bias the results.

EFFECT OF BEAM SEPARATION ON THE LIDAR/RADAR BACKSCATTER RATIO

We shall consider a 1-second averaging time for the spaceborne radar and lidar to achieve sufficient sensitivity, which results in a pixel length of 7 km. The effect of footprint separation has been simulated using 64 synthetic cloud fields generated by the procedure described in the previous section. The footprint of the lidar was taken as 100 m and that of the radar to be 700 m with both instruments having a Gaussian beam pattern. Calculating the radar backscatter is relatively straightforward, but to calculate the lidar backscatter the radar reflectivity field was transformed to an optical extinction using an empirical relationship from Hogan and Illingworth (1999) and then a constant extinction to backscatter ratio was assumed for the ice cloud to calculate the lidar backscatter field. Because we are only interested in the change in the radar/lidar backscatter ratio with footprint separation the exact choice of the constant value of the extinction to backscatter ratio is immaterial.

The swaths of the spaceborne radar and lidar were offset by up to 10 km in the direction parallel to the satellite motion. The resultant mean fractional error in the backscatter ratio as a function of the separation distance is displayed in Fig. 3. Note that even when the centres of the footprints are both co-located there is an error in the backscatter ratio because the radar footprint is larger than that of the lidar, but the rms value of this error is only 0.2 dB, or less than 5%, so can be neglected. When the footprint separation distance reaches 5 km then the error approaches 3 dB, or a factor of two, and this is unacceptable.

CONCLUSIONS

A spaceborne cloud radar and lidar have been 'flown' over synthetic cloud fields having the same spatial characteristics and variability as those observed by ground based radars, and the change in the apparent radar/lidar backscatter ratio has been calculated. Even with perfectly co-located footprints there is a small error in the backscatter ratio because the lidar footprint is 100 m is less that the 700 m radar footprint, but this error is less than 5% and can be neglected. When the tracks of the footprints of the two instruments are 5 km apart then the mean error in the backscatter ratio approaches a factor of two, which is unacceptable. The simulations are idealised and in practice the degradation will be greater than calculated. Firstly, and most importantly, it has been assumed that the lidar backscatter signal is unattenuated, but in practice it will be heavily attenuated and a correction for such attenuation must be made. Gate-by-gate correction algorithms are notoriously unstable, and so the most reliable attenuation correction algorithms use the radar reflectivity profile as a first guess to constrain the extinction profile (see other CLARE papers). Clearly, if the first guess constraint is taken from a radar profile some distance from the lidar profile there is no guarantee that this correction procedure will converge to a stable solution. Further simulations would be needed to quantify this effect. A second effect is the time separation of the two platforms. If they are separated by (say) one minute, then cirrus clouds moving at (say) 30 m s^{-1} could lead to a further spatial separation of up to 2 km and of course their structure could also evolve.

The conclusion of this analysis is that flying the radar and lidar on separate platforms would lead to an unacceptable degradation in the derived radar/lidar backscatter signal.

ACKNOWLEDGEMENTS

The radar data were provided by the Radiocommunications Research Unit at the Rutherford Appleton Laboratory.

REFERENCES

Danne, O., G. G. Mace, E. E. Clothiaux, X. Dong, T. P. Ackerman and M. Quante, 1996: Observing structures and vertical motions within stratiform clouds using a vertical pointing 94-GHz cloud radar. *Beitr. Phys. Atmosph.,* **69**(1), 229–237.

Hogan, R. J., and A. J. Illingworth, 1999: The potential of spaceborne dual-wavelength radar to make global measurements of cirrus clouds. *J. Atmos. Oceanic Tech.,* **16**(5), 518–531.